INVESTIGATION OF AN ELECTROMAGNETIC UNDERWATER COMMUNICATIONS SYSTEM

by

Douglas W. White

Submitted in Partial Fulfillment

of the Requirements for the

Degree of Bachelor of Science

at the

MASSACHUSETTS INSTITUTE OF TECHNOLOGY

January 1975

Signature of Author . . . . . .
Department of Electrical Engineering, January 22, 1975
Department of Physics, January 22, 1975

Certified by . . . . . .
Thesis Supervisor

Accepted by . . . . . .
Chairman, Departmental Committee on Theses

MAY 23 1975
LIBRARIES

Investigation of an Electromagnetic Underwater Communications System

by Douglas W. White

Thesis Advisor, Charles Miller, Lecturer

ABSTRACT

This thesis investigated the properties of an electromagnetic underwater communications technique which establishes a propagating electric field in water using an audio frequency current passed between two submerged electrodes separated by a short distance. This field is then picked up at a distance by a second pair of electrodes and fed to an amplifier (the receiver).

Two research groups have investigated this system in the past, claimed excellent results and then abandoned it for no apparent reason. In this thesis, the fields were first analyzed theoretically and then experimentally in an effort to verify the results, and possibly to determine why it was abandoned if it works as well as was claimed.

The experiments (conducted in the MIT swimming pool) supported the accuracy of the theoretical analysis, and showed no reason for the earlier claims. Although some improvements to the methods used could be made, this system appears to have no practical advantage over acoustic communications systems now in use.

ACKNOWLEDGEMENTS

I wish to express my thanks to all of my many friends who assisted me with the experiments and my special thanks to advisor Charlie Miller, Professor Haus and Professor Staelin for their assistance with the theoretical sections, and Professor Carmichael, Albert Bradley and the other members of the Ocean Engineering Department Summer Laboratory who helped with many of the countless details that go into such a project.

TABLE OF CONTENTS

LIST OF FIGURES

INTRODUCTION

In recent years, there has been a steady increase in scientific and industrial activity underwater. This has brought with it a growing need for a simple and reliable method of underwater communications. Acoustic communications has been used extensively in underwater work, but limited bandwidth and susceptability to interference from noise, scattering, and reflections tend to limit its usefulness. Ordinary electromagnetic radiation is relatively free from this sort of interference, but it attenuates rapidly in water except at very low frequencies, where it has been used for submarine communications.

During World War II, the Office of Scientific Research and Development investigated a short range communications system using audio frequency currents fed through the water. A dipole antenna, consisting of two electrodes separated by a short distance, was used to establish the current, and a similar dipole was used to detect the electric field produced. Ranges up to 1,500 meters were achieved with relatively simple equipment, and no problems with any sort of interference were encountered. Although the final report was optimistic about the usefulness of such a system, the Government abandoned it for unknown reasons.

This system of communicating was apparently rediscovered in 1964 by Wallace A. Minto, who made a number of impressive claims about its effectiveness, including transmissions up to 30 miles. He also claimed that it involved a new form of radiation, which does not obey accepted electromegnetic theory. Although he was very secretive about his methods, his equipment was very similar to the type used by the O.S.R.D. in the 1940's, and it is reasonable to assume that Minto was actually using the same technique. Despite his original claims, Minto also abandoned his work on this system.

The purposes of this thesis were to determine, first by theoretical analysis and then by experimental measurements, how this type of communications works, and whether or not the signal propagation obeys currently accepted theory. Once the characteristics of the system are understood, it should be possible to determine if the system has any particular advantages over acoustic systems, and possibly why it has been abandoned twice despite impressive claims as to its effectiveness.

The fields for the unbounded case were analyzed using a short dipole model for the antennas, and the effects of nearby boundaries on the fields were determined using the concept of image charges. A preliminary series of experiments was then performed to study the electrical properties of the medium to facilitate the design of the equipment to

be used for the actual propagation measurements. Next, several antennas and three small transmitters were constructed, and a series of field propagation experiments was performed in the MIT swimming pool. The transmitters' power levels were kept sufficiently low that a good simulation of long distance and deep water transmissions could be done in the confines of the pool. Measurements were made of the effects of varying transmission frequency and antenna length, depth, separation and orientation. The results were then compared with the field equations derived at the beginning, and with the claims of the earlier researchers.

The measurements confirmed the applicability of the field equations, and tend to refute the claims made by the O.S.R.D. researchers and Minto. The fields attenuate very rapidly with distance, and appear to offer no particular advantage over current acoustic systems, although there are slightly more efficient methods of using this type of communication than were actually tested.

THEORETICAL ANALYSIS

The transmitter consists of a low impedance audio frequency (less than 100 kHz) source connected to a pair of conducting electrodes separated by a short distance (one meter or less). This antenna is submerged in the water, and an electric field is produced in the water along with an electric current. The receiving antenna, which is similar to the transmitting antenna, produces a voltage when it is aligned along the electric field lines produced by the transmitter. For maximum efficiency, the receiver should be matched to the low impedance of the receiving antenna. However, for experimental measurements the receiver should have a very high impedance to avoid perturbing the field.

In order to analytically calculate the fields produced, the simplest approach is to model the transmitting antenna as an infinitesimal current source. This model should be reasonably accurate as long as the length of the antenna is fairly short compared to the wavelength of the signal in the water.

The equation for the voltage produced across a high impedance receiving antenna using this model (derived in Appendix I) for the geometry shown in Figure 1 is:

$$V = \frac{I_0 d_1 d_2 e^{-\gamma' r}}{4\pi\sigma r^3} (1 + \gamma' r)(2 \cos\theta \cos\theta' + \sin\theta \sin\theta') \cdot \cos(\omega t - \gamma' r), \quad (1)$$

where V is the r.m.s. voltage at the receiver,

I_0 is the r.m.s. transmitter antenna current,

d_1 is the length of the transmitting antenna,

d_2 is the length of the receiving antenna,

r is the antenna separation in meters,

σ is the conductivity of the water,

θ is the transmitting antenna angle (see Figure 1),

θ' is the receiving antenna angle (see Figure 1),

ω is the angular frequency of the signal, and

γ' is a propagation constant given by

$$\gamma' = \sqrt{\frac{\omega\mu\sigma}{2}}$$

where μ is the magnetic permeability of the water.

Several things are apparent from this equation. First, and most important, is that both the expected dipole (r^{-3}) and radiation (r^{-2}) terms are present with the exponential decay $e^{-\gamma' r}$ characteristic of signal propagation in lossy media. Also, maximum transmission should occur

with the antennas in line with each other rather than parallel to each other as is ordinarily the case for dipole antennas. There are no unexpected terms, and none that would indicate any unusual radiation characteristics.

Equation (1) also implies that the signal propagates with an effective wavelength equal to 2π times the skin depth δ defined by

$$\delta = \frac{1}{\gamma'} . \tag{2}$$

At 1 kHz, this gives a wavelength of about 1,400 meters in fresh water ($\delta \approx 5\ 10^{-3}$ mhos/m), or about 50 meters in salt water ($\delta \approx 4$ mhos/m). This means that any salt water experiments must be designed carefully to ensure the validity of the short dipole approximation used to derive Equation (1). If the antenna length is increased past about one-fiftieth of a wavelength, the signal strength will peak at odd multiples of one-half a wavelength, and almost completely vanish at even multiples of a half wavelength. Because of the practical difficulties of working with an electrically long fresh water antenna, detailed calculations were restricted to the short dipole model, which could be used (with some limitations) for both fresh and salt water transmissions.

Thus far, the analysis has been limited to the unbounded case. Any restriction of the current flow by insulating boundaries, such as the surface, will tend to

increase the field everywhere in the water. In the extreme case where the system is being used in shallow water over a bottom with a low conductivity, the problem becomes roughly two-dimensional and the fields will propagate with an r^{-1} and an r^{-2} dependence.

The problems of only one boundary can be easily analyzed using the concept of an image antenna. The field from the transmitting antenna with a boundary nearby can be duplicated by adding the field of a second "image" antenna to the field produced in the unbounded case. The image antenna for an insulating boundary of this sort (derived in Appendix II) is in phase with the transmitting antenna and located a distance $2d$ away, where d is the distance from the boundary to the transmitting antenna (see Figure 2). For this geometry, the voltage at the receiver is given by:

$$V = \frac{I_0 d_1 d_2}{4\pi\sigma}\left[\frac{2\, e^{-\gamma' r}\,(1+\gamma' r)\cos(\omega t-\gamma' r)}{r^3} + \frac{e^{-\gamma' r'}\,(1+\gamma' r')\,(\cos^2\alpha+1)\cos(\omega t-\gamma' r')}{r'^3}\right] \tag{3}$$

where

$$r' = \sqrt{4d^2 + r^2} \tag{4}$$

and

$$\alpha = \arctan\frac{2d}{r}\ . \tag{5}$$

In the case where the transmitting and receiving antennas are quite deep, the effect of the image antenna is

fairly small. However, if the transmitting antenna is operated just under the surface, the voltage produced is exactly double that of the unbounded case. Although this will not produce any large increase in the effective range of the transmission, it shows that boundaries should not be completely ignored when precise measurements are being made.

It would be helpful if some sort of comparison could be made between this analysis and those made by past researchers. Unfortunately, the derivation of the equations in the O.S.R.D. report is not available, and Mr. Minto apparently avoided the theoretical side of the problem entirely. The describing equation from the O.S.R.D. report is given below in a slightly rearranged form to make comparison easier.

$$V = \frac{I_0 d_1 d_2}{2\pi\sigma r^3}\Big[(2\sin\theta\sin\theta' - \cos\theta\cos\theta')\cos\omega t - e^{-\gamma' r}(\cos\theta\cos\theta' + \sin\theta\sin\theta')(1+\gamma' r) \cdot \cos(\omega t - \gamma' r)\Big] \tag{6}$$

Equation (6) contains one major difference from Equation (1). The first term inside the large brackets implies the existence of an electric field with no exponential decay, no dependence on frequency, and no spatial phase shift with respect to the source. This term implies the instantaneous transmission of information, which is relativistically impossible. It is clear that some sort of error was

made in the original derivation, but it is impossible to determine where from the information presented in the report.

If Equation (1) is accurate, it is quite simple to determine whether or not this is a practical system of communication. For example, at 1 kHz in sea water with one meter antennas and a one ampere antenna current, the voltage at the receiver should be 1.4 microvolts at 20 meters, and 2 picovolts at 100 meters (versus 4 microvolts and 40 nanovolts predicted by Equation 6). If the experimental equations verify Equation (1), it would appear that the system is only useful for ranges less than one or two hundred feet.

Figure 1

Basic Transmitting Geometry

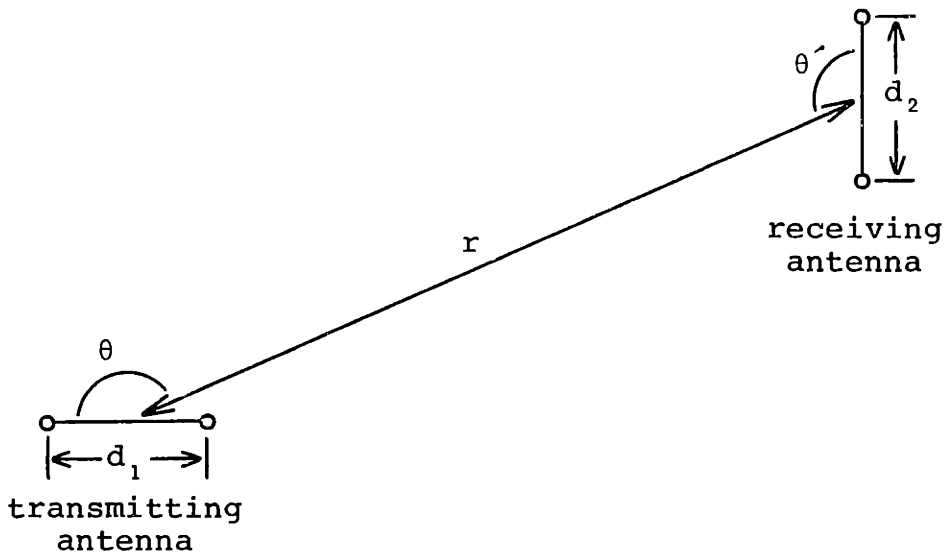

Figure 2

Transmitting Geometry with an Insulating Boundary

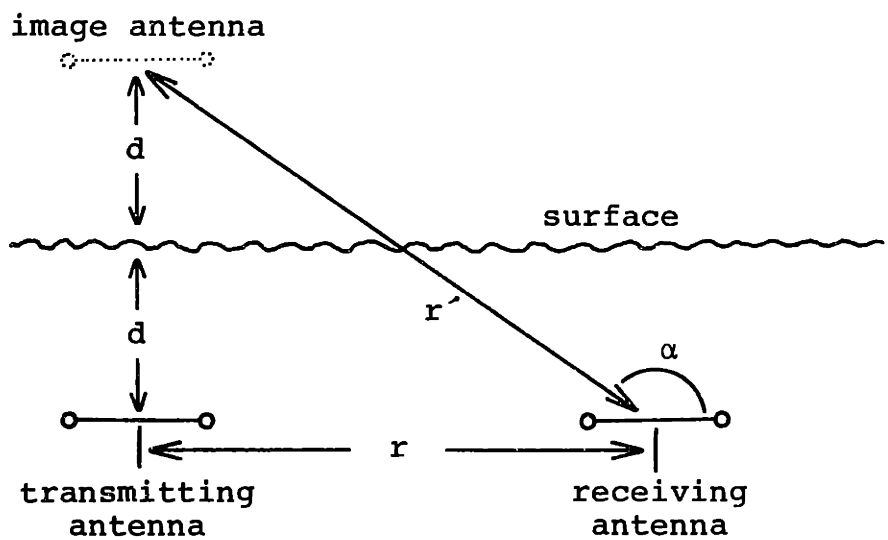

PRELIMINARY EXPERIMENTS

Before any serious transmitter or receiver designs could be worked on, it was necessary to measure the characteristics of various antenna structures. This assisted in selecting an optimum antenna design, and in properly matching the transmitter to the antenna impedance.

The equation for the voltage developed across the receiving antenna shows a linear increase with both length and driving current of the transmitting antenna. For maximum efficiency, it is desirable to have as low an antenna impedance as possible. At a fixed current level, and therefore a fixed voltage at the receiver, halving the antenna impedance halves the power drain on the transmitter.

Measurements were taken of antenna impedance as a function of length, electrode area, and driving frequency. The length and area impedances were measured with a 1 kHz impedance bridge. The frequency measurements were made by displaying the actual voltage-current curves on an oscilloscope using a buffered signal generator and a current probe.

As the antenna length is increased beyond a few times the electrode dimensions, the impedance increases rapidly and then levels off to a fairly slowly increasing function. Because the field strength is directly proportional to an-

tenna length and driving current, this means that the field can be increased by lengthening the antenna without requiring a proportional increase in transmitting power. Therefore, for maximum efficiency, the antennas should be made as long as practically possible up to about one-fiftieth of a wavelength, where the short dipole model begins to break down severely.

It was found that increasing the electrcde area beyond three or four square inches (using copper sheet) gave only a very gradual decrease in impedance. Once the electrodes are larger than this, it takes a considerable increase in area to make much difference in the impedance. The electrodes finally settled on were made from one and one-half inch diameter copper pipe to give as much area as possible in a small volume.

The antenna impedance was almost purely resistive and fairly constant at high frequencies (greater than 1 kHz). However, at very low frequencies (several Hz), electrochemical effects gave a rapid increase in both resistance and phase shift. If the d.c. resistance of an antenna is measured with an ohm meter, the reading will drift fairly rapidly up to a considerably higher value than the impedance of the same antenna at 1 kHz. For this reason, transmissions should be done at frequencies higher than at least 100 Hz, and a.c. coupling should be used whenever possible.

EQUIPMENT

Originally, most of the important measurements were to be taken in sea water by divers, and a considerable amount of work was put into developing a transmitter and receiver for this purpose. Unfortunately, this work had to be abandoned after a number of circuit and waterproofing problems threatened to delay the experiments excessively. Therefore, all of the actual measurements were done in the MIT swimming pool.

There were two basic antenna designs used. The antennas used for the antenna pattern measurements consisted of two 1¼ inch square copper plates bolted (using nylon hardware) to ten inch by one-half inch diameter acrylic plastic rods. The antennas used for the remainder of the experiments were made with two three inch sections of the copper pipe mentioned earlier fastened to one-half meter lengths of plastic rod. These electrodes were held in place with small elastics, to allow changing the electrode separation. The small antennas were supported three feet off the pool bottom with acrylic rods placed in polyvinyl-chloride (pvc) bases. The longer antennas were suspended by acrylic rods from a floating plank for the attenuation with length and depth measurements, and suspended from styrofoam floats for the distance and frequency response mea-

surements.

The transmitter used for the antenna pattern experiments was made with two 741 operational amplifiers: one as a 10 kHz oscillator, and the second as a buffer amplifier (see Figure 3). This was housed in a small watertight pvc cylinder, and was battery powered to eliminate power cables from the surface. The electrical connections to the antenna were made with a pair of epoxy-filled pin plugs sealed in short pieces of soft pvc tubing.

Because variations in antenna impedance would cause variations in the field strength if a normal voltage source transmitter were used, two current source transmitters were used for the remainder of the experiments. The first circuit was used for the antenna depth and antenna length experiments. It consisted of a 1 kHz oscillator (similar to the 10 kHz oscillator used in the small transmitter) driving a 10 milliampere a.c. current source made with an LM301A operational amplifier (see Figure 4). The LM301A has a standard double pole frequency compensation, and a provision for eliminating the d.c. component of the output. This must be done by adjusting the amplifier offset, because the load is in the actual feedback path, and cannot be isolated with capacitors (although a transformer could be used). The second current source transmitter was designed to be used with an audio signal generator for the distance and frequency response measurements. The actual

current source is identical to the first one, except that it uses feedforward compensation to improve the frequency response of the amplifier (see Figure 5). The 600 ohm input is designed to match the signal generator impedance, and is adjusted to give 10 milliamperes output for a one volt input.

The receiver used for all of the experiments was actually a Hewlett Packard model 403B a.c. voltmeter. This can measure voltages down to .1 millivolt full scale, at frequencies up to 4 MHz .

The conductivity of the pool was also measured with a commercial instrument. The unit used was a Radiometer Copenhagen Conductivity Meter, and the calibration was checked with a one-tenth and a one-one-hundredth molar solution of potassium chloride.

Figure 3

10 kHz Transmitter Schematic

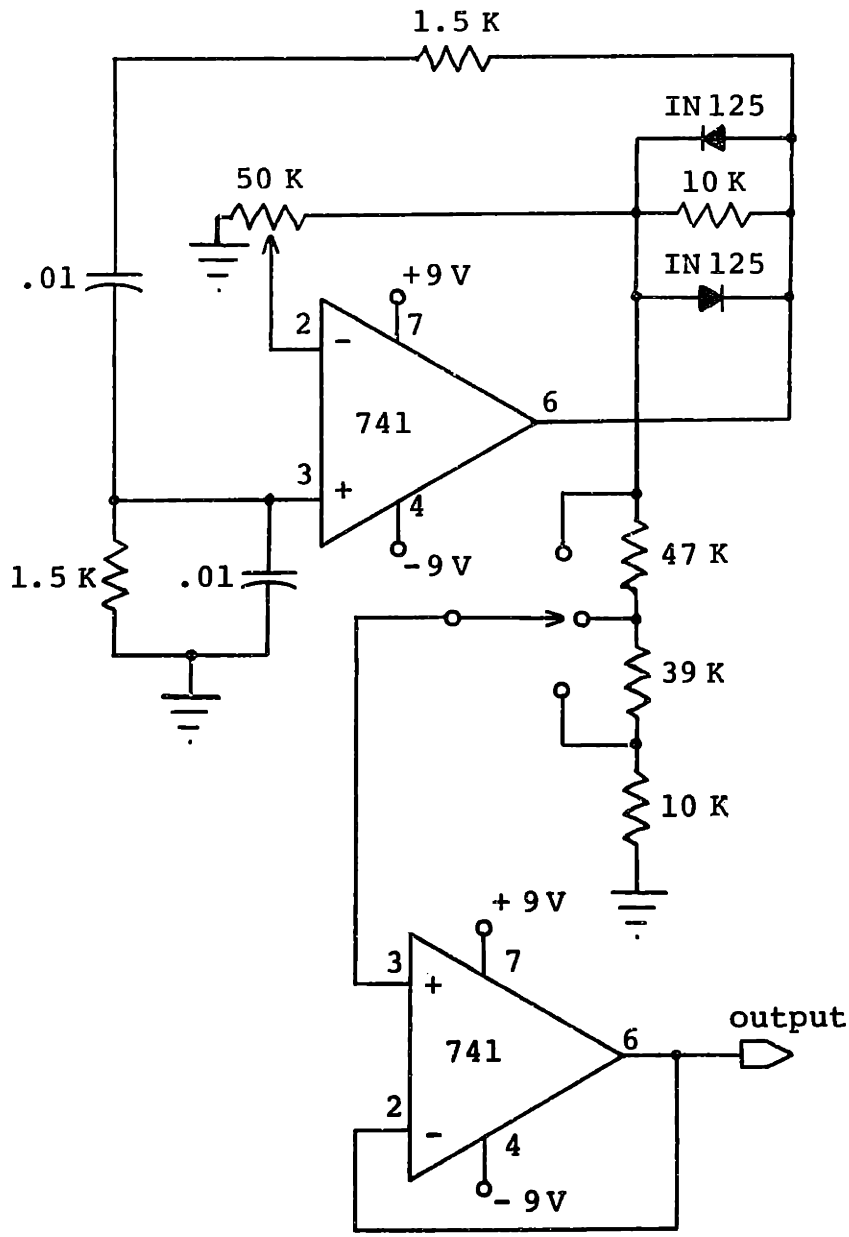

Figure 4

1 kHz Current Source Transmitter Schematic

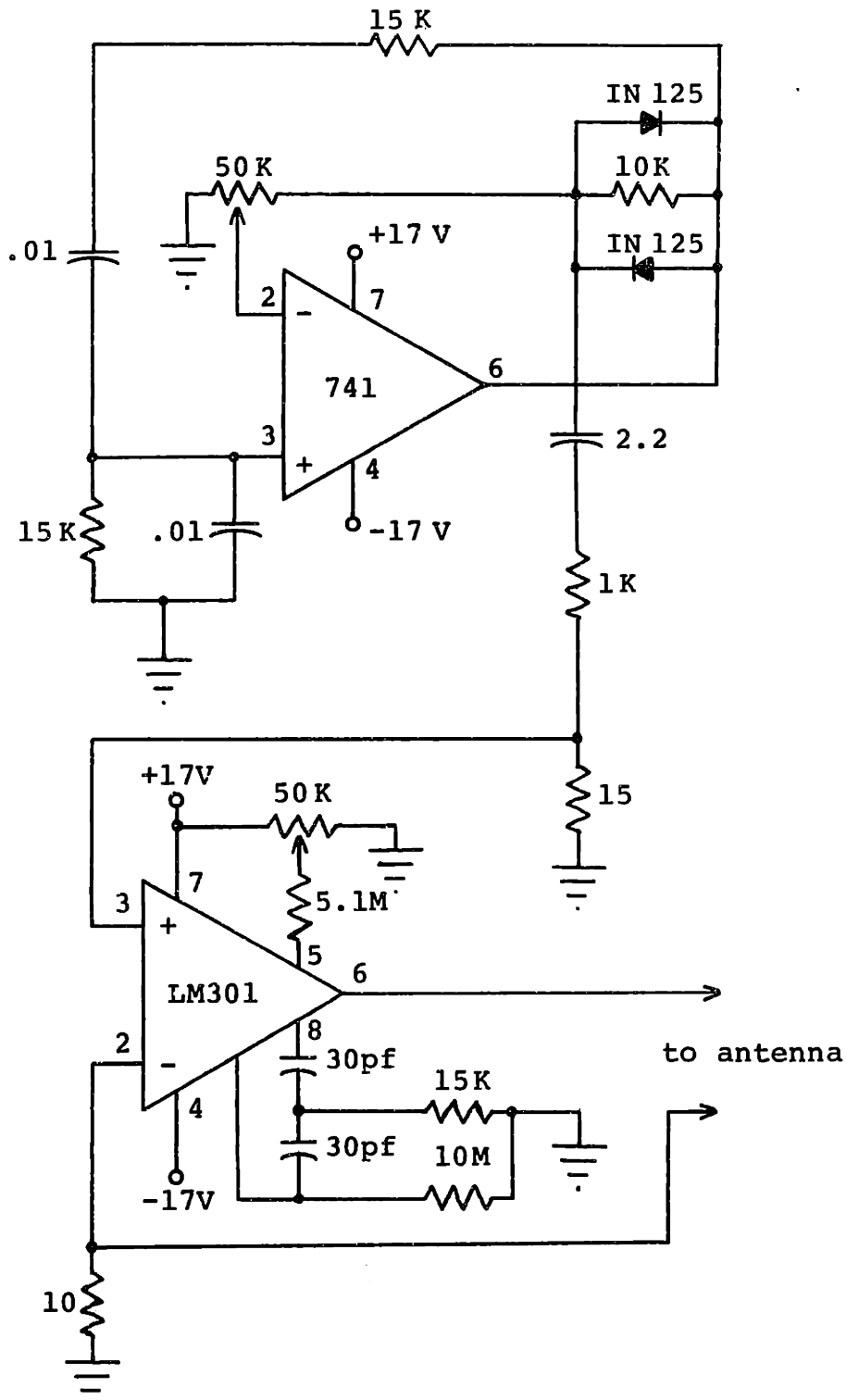

Figure 5

Broadband Current Source Transmitter Schematic

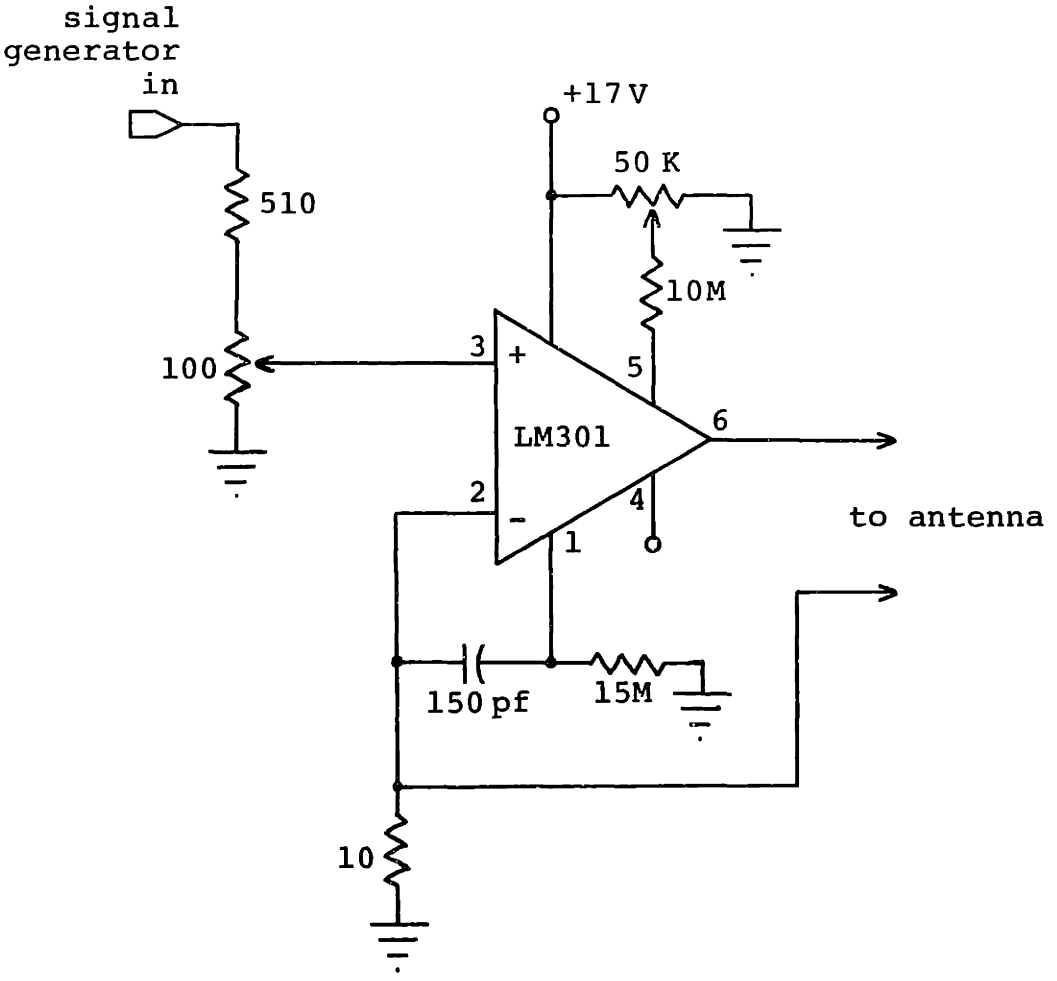

EXPERIMENTS

Five major experiments were performed to measure the propagation characteristics of the system:

(1) measurement of the angular dependence of the fields;

(2) measurement of the effects of depth on transmission;

(3) measurement of field strength with changing antenna length;

(4) measurement of field attenuation with distance, and;

(5) measurement of the frequency characteristics of the transmission.

The antenna pattern experiment was performed with the small 10 kHz transmitter, and because there was no readily available method of measuring the exact antenna current, the data was normalized to a peak value of one to compare it with the theoretical values rather than plotting actual field levels. A radial plot of the field pattern for $\theta' = 0$ and the corresponding theoretical pattern are shown in Figure 6. The field pattern for $\theta' = 90°$ was similar, only rotated 90° and of half the amplitude of the $\theta' = 0$

plot as was theoretically predicted.

At the time the subsequent measurements were taken, there was no available method for determining the pool's conductivity. It was assumed that the conductivity would be relatively constant, and could be measured at any time. Unfortunately, when several experiments were performed on different days, the measurements showed variations under otherwise identical conditions that could only be explained by fluctuations in the pool's conductivity by as much as a factor of two. After the experiments were completed, a conductivity meter was located, and a check was made to be certain that the measurements were at least close to the theoretical values. The measured value was 2.54 mhos/meter . The graphs for the attenuation with depth (Figure 7) and attenuation with distance (Figure 8) contain theoretical curves for values of σ a factor of two above and below this value for comparison with the experimental data.

When the salt water experiments were abandoned and it was decided to perform the measurements in the MIT pool, it became important to have some idea of how the insulating surfaces of the pool would affect the fields. Using one-half meter antennas at 1 kHz , the received signal was measured as both antennas were lowered into the center of the pool. A plot of the results is shown in Figure 7 along with the theoretical curves for σ = .127 mhos/meter and σ = .504 mhos/meter . The signal strength for small and

large depths is within the correct region for the estimated conductivities, but at intermediate depths the signal rolls off considerably faster than predicted. This is probably the result of a distortion of the antenna pattern caused by the large electrodes used on the antennas. The antenna used for the antenna pattern experiments had much smaller electrodes, and probably made a much better approximation to a small current source at the separation used (two meters) than the larger antennas. The important points are that the field falls off very quickly, and that it is twice as strong at the surface as it is deeply submerged. These allowed the remaining experiments to be done with the antennas just under the surface without the need for waterproof electronics, and without worrying about the effects of the other boundaries. The final results were then divided by two to get the deep water field for comparison with the theoretical calculations.

The measurements of field strength dependence on length showed that they are directly proportional to each other, just as predicted. The relationship was completely linear from an antenna length of one-half meter to one-quarter meter where noise began interfering with the readings. The actual measurements were done by varying the transmitting antenna length, but the results must also hold for the receiving antenna because of reciprocity considerations.

The attenuation with distance is graphed in Figure 8 along with the theoretical curves for the estimated range of the pool's conductivity. Apparently the conductivity of the pool when this measurement was done was very close to the 2.54 mhos/meter measured later, because the experimental curve lies almost exactly half-way between the two theoretical curves.

In an effort to reduce the effects of noise on the measurements, the frequency response experiment was performed at an antenna separation of two meters. Unfortunately, before the signal began to fall off at this distance (the important parameter being $r\gamma'$), the frequency was high enough to start violating the short dipole premise that the theory is based on. Above 20 kHz the antenna was long enough (electrically) to begin to behave more and more like a resonant half wavelength antenna than a short dipole. The response was flat up to this point, and then slowly began to increase, continuing past the limit of the signal generator (100 kHz). Using a conductivity of .25 mhos/meter, 20 kHz corresponds to a wavelength of about 45 meters, where a one-half meter antenna should still be a good approximation to a short dipole. At 100 kHz , the wavelength is about 20 meters and the model is no longer very valid. The antennas are not fully resonant (one-half a wavelength) until over 150 MHz , but the effect prevented any accurate frequency decay measurements from being made.

Figure 6

Antenna Pattern Plot

Field Strength Plotted Radially
and Normalized to 1
(one major radial division = .25)

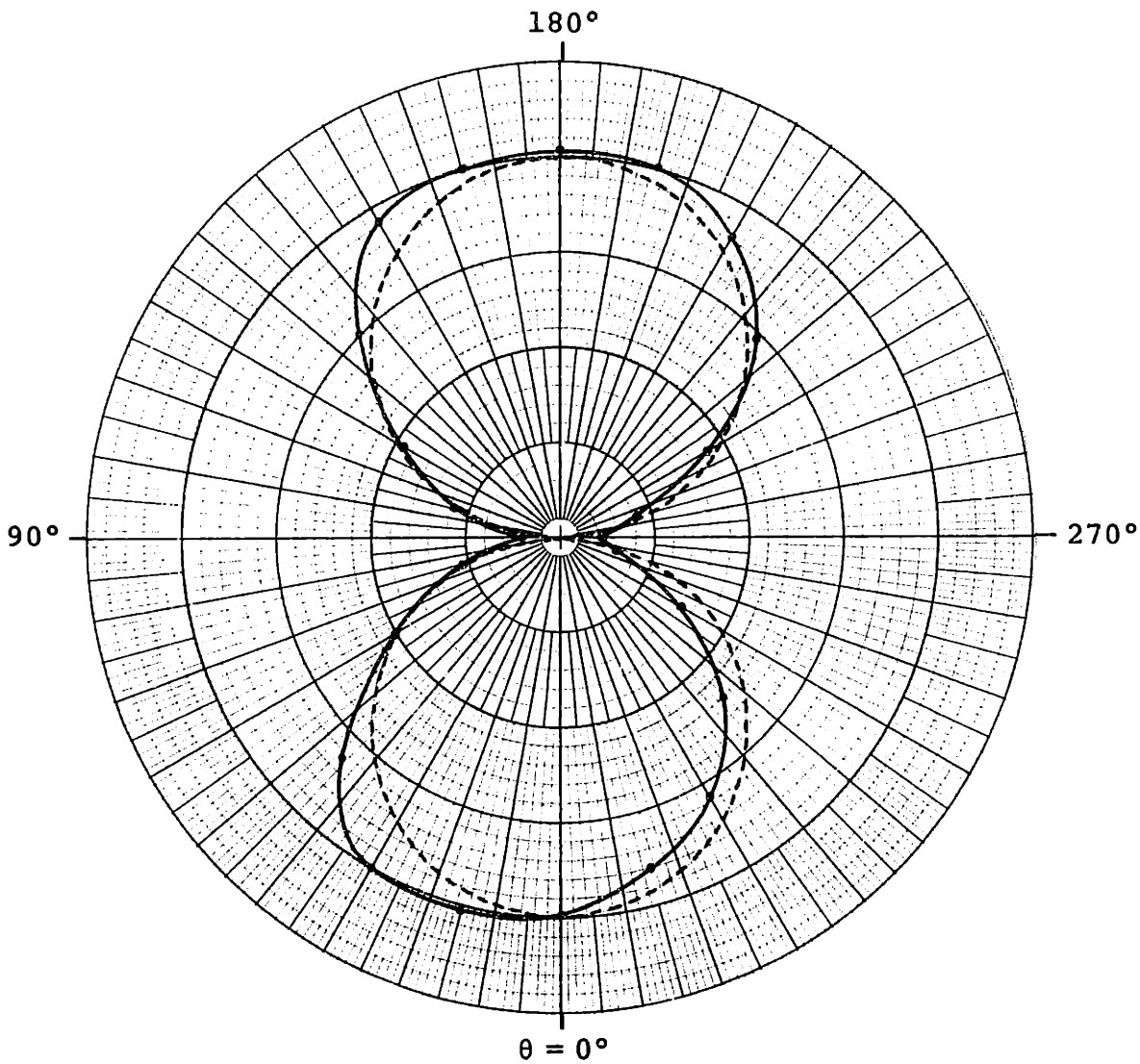

------- theoretical values for $\theta' = 0$

_____ experimental values for $\theta' = 0$

Figure 7

Field Attenuation with Depth

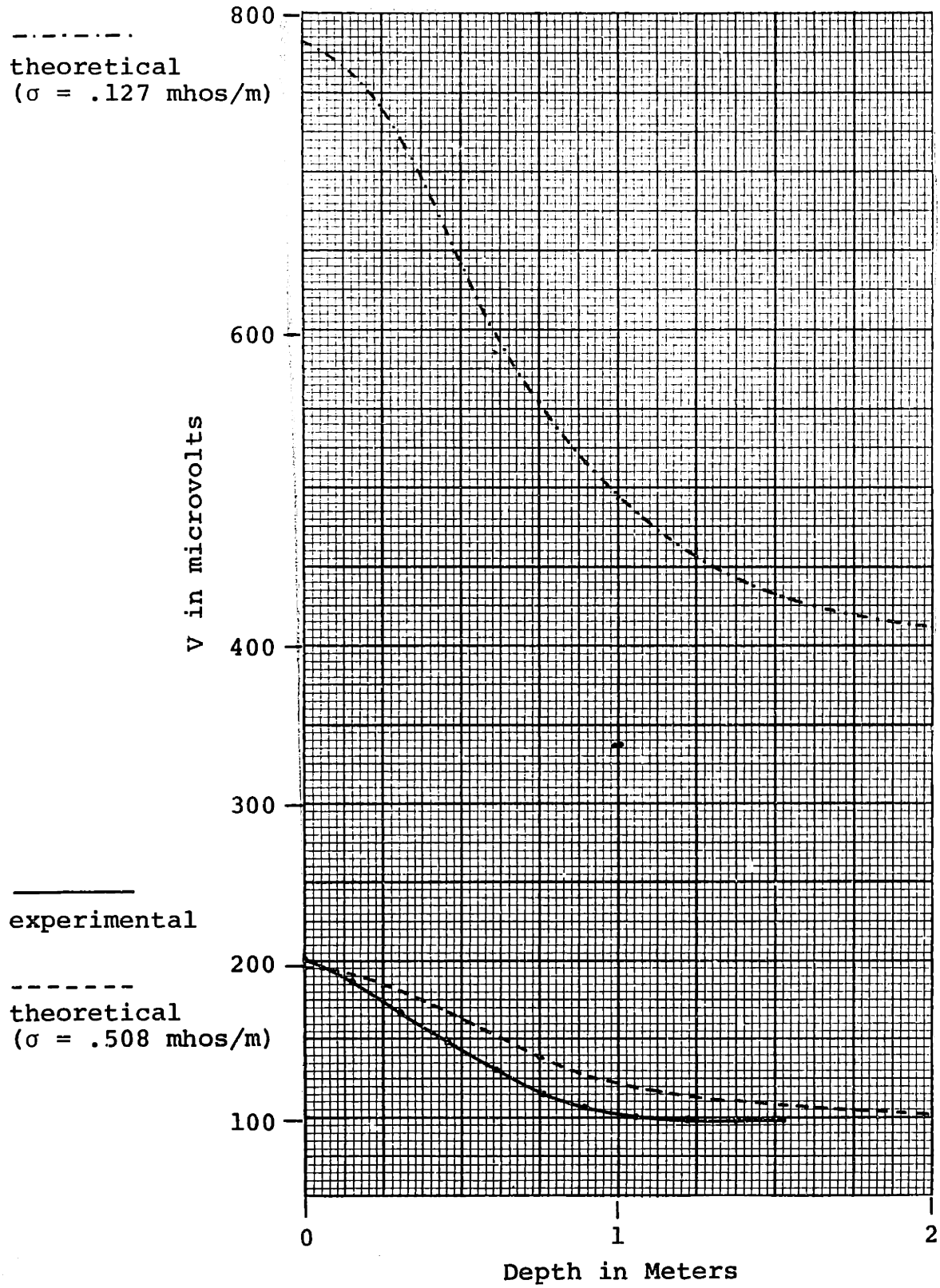

Figure 8

Field Attenuation with Distance

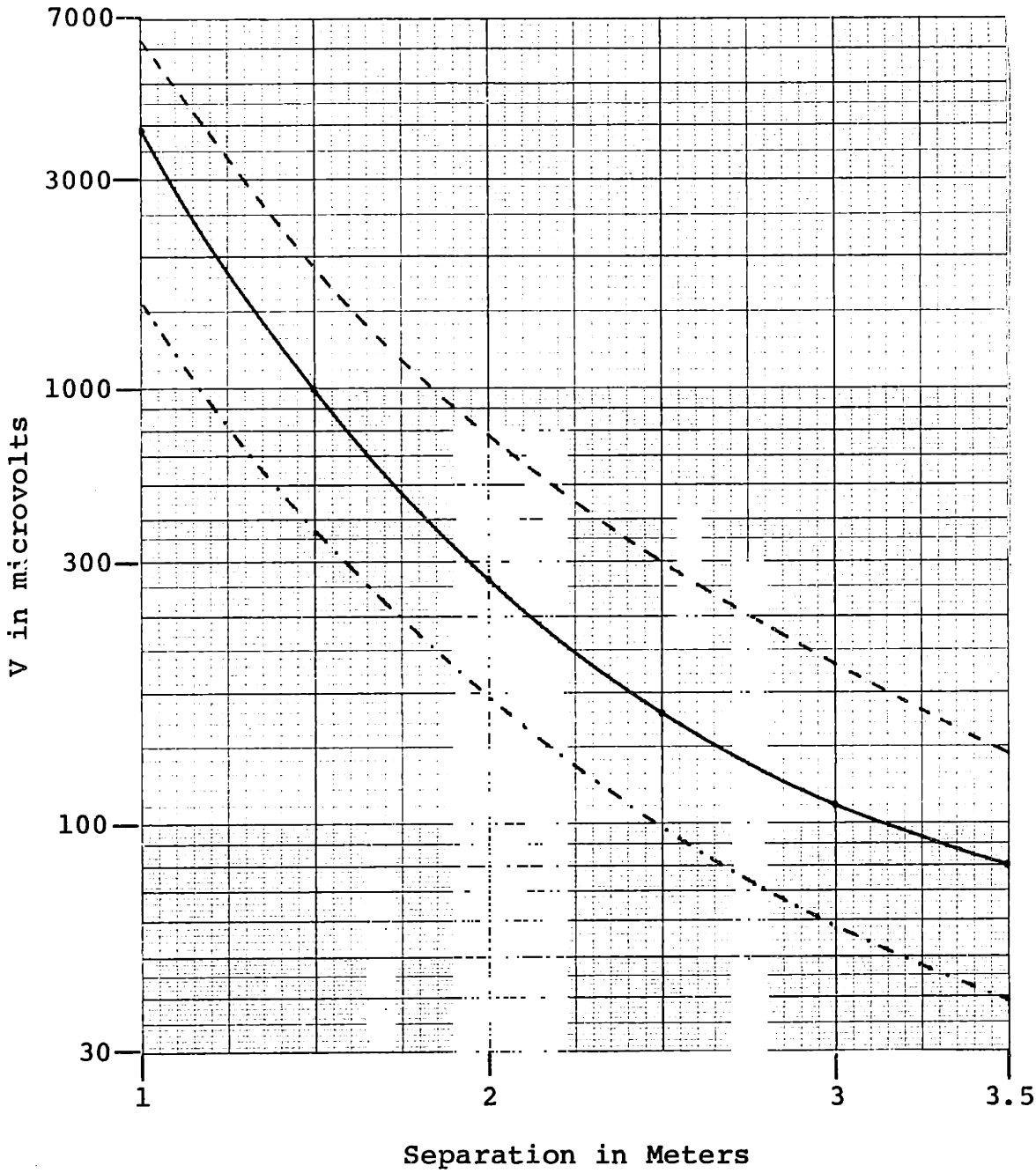

CONCLUSIONS

Within the limitations of the short dipole model, and in spite of the uncertainties in the conductivity, the experiments appear to justify the applicability of the theoretical analysis of this communications method. There is no strong evidence of anything unusual going on as Mr. Minto claimed, and the field equation given in the Office of Scientific Research and Development report has already been shown to be physically impossible from relativistic considerations.

Unfortunately, if the analysis is correct, there seems to be little hope of this ever becoming a particularly useful form of communications. In sea water especially, the fields will attenuate so rapidly with distance that only extremely low frequencies could be used over distances greater than fifty meters. It is possible that going to a resonant antenna and matching the receiver to the antenna to increase efficiency would increase this figure to a hundred meters or more, but the O.S.R.D. claim of a transmission of 1,500 meters and Minto's claim of a range of thirty miles are very hard to believe.

Before this approach to underwater communications is completely abandoned, a careful investigation of the resonant antenna equations and the possibilities of improved an-

tenna coupling should be conducted. It is also possible that it might be useful for fresh water systems even if it proves useless for salt water systems.

Even if this type cf system proves completely useless for communications, it may have other uses. The distortion of the fields near boundaries of changing conductivity may be useful for geologic analysis of the sea bottom, or for some sort of metal detector.

APPENDIX I

For frequencies where the antenna is short compared to a wavelength in water, the antenna can be modeled as a current impulse at the origin (see Figure 9). This has a current density $\underline{\bar{J}}$ ($\bar{}$ indicates a vector, $\underline{\ }$ indicates that it is complex) given by:

$$\underline{\bar{J}} = (\underline{I}\, d_1)\, \delta_3 (\bar{r})\, \bar{i}_z \ , \tag{1}$$

where

$$\underline{I} = I_0\, e^{j\omega t} \ , \tag{2}$$

ω is the angular frequency of the signal,

d_1 is the length of the transmitting antenna, and

$\bar{r}$ is the radius vector.

In a dissipative medium such as water, this will produce a vector potential $\underline{\bar{A}}$ defined by:

$$\underline{\bar{A}} = \frac{\mu\, \underline{I}\, d_1\, e^{-\gamma r}}{4\pi r}\, \bar{i}_z \ , \tag{3}$$

where $r = |\bar{r}|$,

μ is the magnetic permeability of the water, and

γ is a propagation constant.

For the high loss case of water, γ is approximately given

by:

$$\gamma = (1 + j)\sqrt{\frac{\omega\mu\sigma}{2}} = (1 + j)\,\gamma' \ , \tag{4}$$

where σ is the water's conductivity.

The easiest way to determine the electric field $\underline{\bar{E}}$ is by first calculating the magnetic field $\underline{\bar{H}}$ from $\underline{\bar{A}}$. It also simplifies matters to convert to spherical coordinates (see Figure 10) using the identity:

$$\bar{i}_z = \bar{i}_r \cos\theta - \bar{i}_\theta \sin\theta \ . \tag{5}$$

Substituting Equation (5) into Equation (3) gives:

$$\underline{\bar{A}} = \frac{\mu \underline{I}\, d_1\, e^{-\gamma r}}{4\pi r} \left(\bar{i}_r \cos\theta - \bar{i}_\theta \sin\theta \right) \ . \tag{6}$$

The magnetic field is then given by:

$$\underline{\bar{H}} = \frac{1}{\mu} \nabla \times \underline{\bar{A}} \ , \tag{7}$$

or

$$\underline{\bar{H}} = \frac{\underline{I}\, d_1\, e^{-\gamma r}}{4\pi r^3} (1 + \gamma r^2) \sin\theta\, \bar{i}_\theta \ . \tag{8}$$

The electric field is defined by:

$$\underline{\bar{E}} = \frac{1}{\sigma + j\omega\varepsilon} \nabla \times \underline{\bar{H}} \ , \tag{9}$$

where ε is the dielectric constant of the water.

At frequencies much below one megahertz, the term $j\omega\varepsilon$

is negligible compared to σ in water (this is similar to the approximation already made concerning γ). This reduces Equation (9) to the form:

$$\underline{\bar{E}} = \frac{\underline{I}\, d_1\, e^{-\gamma r}}{4\pi\sigma r^3} \left[2 \cos\theta\, (1 + \gamma r)\, \bar{i}_r + \sin\theta\, (1 + \gamma r + (\gamma r)^2)\, \bar{i}_\theta \right] . \tag{10}$$

The voltage at the receiving dipole is given by:

$$V = Re\, (\underline{\bar{E}} \cdot \bar{d}_2) , \tag{11}$$

where $\bar{d}_2$ is a vector describing the length and orientation of the receiving antenna (see Figure 11). For the geometry shown, $\bar{d}_2$ is given by:

$$\bar{d}_2 = d_2\, (\cos\theta'\, \bar{i}_r + \sin\theta'\, \bar{i}_\theta) . \tag{12}$$

Therefore, the voltage at the receiving antenna is:

$$V = Re \left[\frac{\underline{I}\, d_1\, d_2\, e^{-\gamma r}}{4\pi\sigma r^3} \left\{ 2 \cos\theta \cos\theta' (1 + \gamma r) + \sin\theta \sin\theta' (1 + \gamma r + (\gamma r)^2) \right\} \right] . \tag{13}$$

Substituting in Equation (4) and taking the real part gives the final expression for the receiver voltage at a given point:

$$V = \frac{I_0\, d_1\, d_2\, e^{-\gamma' r}}{4\pi\sigma r^3} (1 + \gamma' r) (2 \cos\theta \cos\theta' + \sin\theta \sin\theta') \cdot \cos(\omega t - \gamma' r) . \tag{14}$$

Figure 9

Transmitting Antenna Model

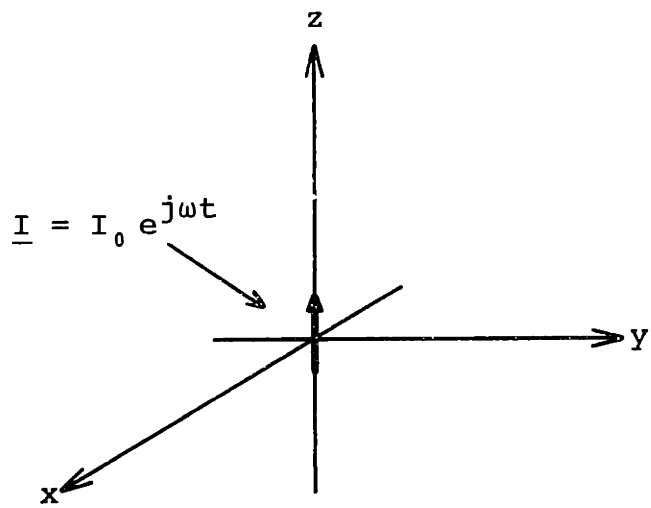

Figure 10

Spherical Coordinates

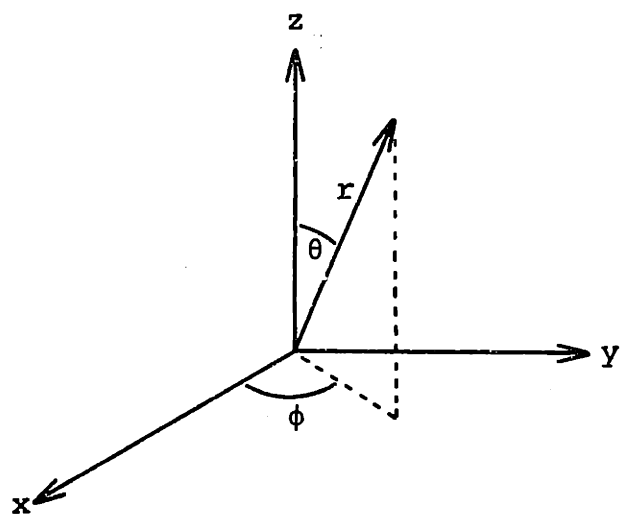

Figure 11

Basic Transmitting Geometry

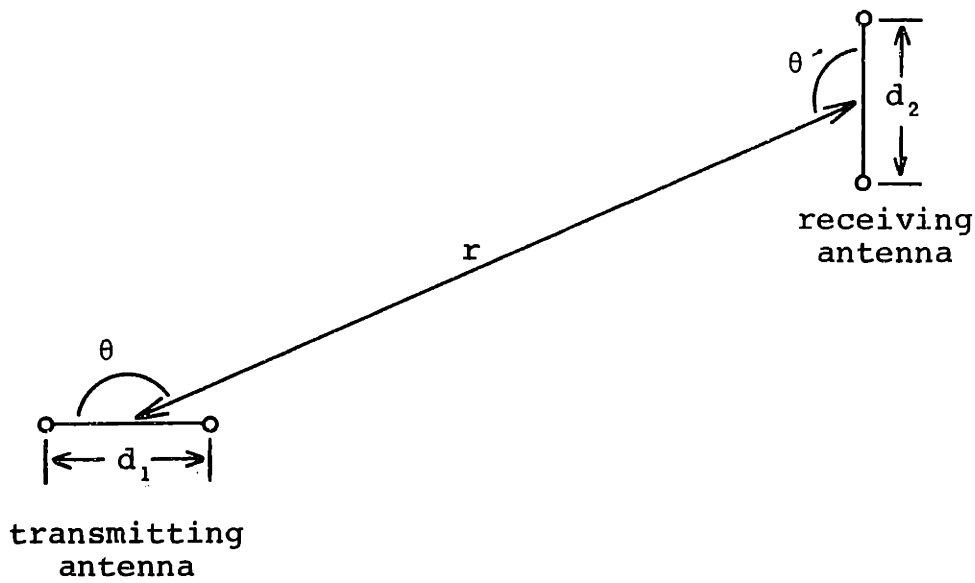

APPENDIX II

The case of transmission near an insulating boundary can be easily analyzed using the image method. The basic geometry of the situation is shown in Figure 12 a . A charge q_r is located in a lossy medium with a complex dielectric constant ξ , a distance d from the boundary with free space. For values of x less than zero, the field can be duplicated by placing an image charge q_{i1} in an infinite lossy medium a distance $2d$ from the original charge (see Figure 12 b). For values of x greater than zero, the field can be duplicated by placing a second image charge q_{i2} in an infinite lossy medium at the location of the original charge (see Figure 12 c). Along the boundary, there are two conditions that the fields must meet. The y component of the electric field must be continuous, and the x component of the electric displacement $\bar{D}$ must be continuous. The first boundary condition gives:

$$\frac{(q_r + q_{i1})\, y}{4\pi\xi r^3} = \frac{q_{i2}\, y}{4\pi\xi r^3} \quad , \tag{1}$$

or

$$q_r + q_{i1} = q_{i2} \quad . \tag{2}$$

The second boundary condition gives:

$$\frac{\xi\,(q_r - q_{i1})\,d}{4\pi\xi r^3} = \frac{\varepsilon_0\, q_{i2}\, d}{4\pi\xi r^3} \quad , \tag{3}$$

or

$$\xi\,(q_r - q_{i1}) = \varepsilon_0\, q_{i2} \quad . \tag{4}$$

Solving Equation (2) and Equation (4) simultaneously for q_{i1} gives:

$$q_{i1} = q_r \left(\frac{\xi - \varepsilon_0}{\xi + \varepsilon_0} \right) \quad . \tag{5}$$

This is the value of the image charge which will duplicate the boundary when placed as in Figure 11 b. In addition, for frequencies below about one megahertz, ε_0 is negligible compared to ξ in water, so

$$q_{i1} = q_r \quad . \tag{6}$$

This means that the correct image antenna for an insulating boundary is one which is identical to the transmitting antenna. The image antenna is in phase with the real antenna and, over short distances, will tend to reinforce the field of the real antenna.

Figure 12

Image Charge Geometries

12 a

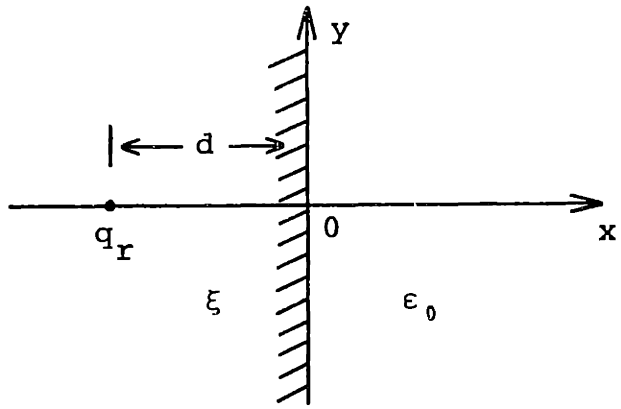

12 b

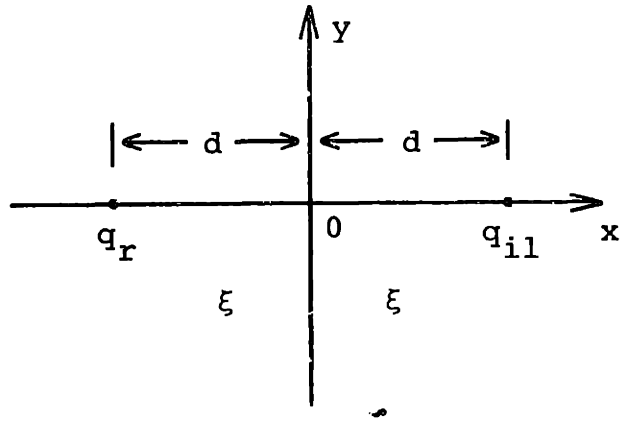

12 c

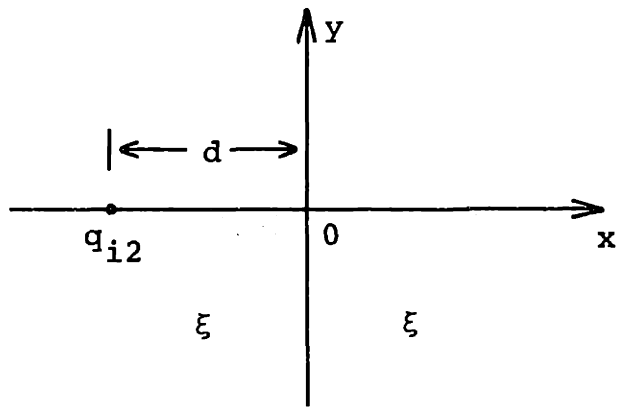

BIBLIOGRAPHY

Briggs, R.J. and R.P. Parker. Electrodynamics: 6.04 Course Notes. Cambridge: Massachusetts Institute of Technology, 1970.

Cowan, E.W. Basic Electromagnetism. New York: Academic Press, 1968.

Hardy, H.C. A System of Short Range Communication by Passing Audio-Frequency Currents Through Water. Philadelphia: University of Pennsylvania, 1945. (Developed under O.S.R.D. Contract No. OEMsr-922.)

Warner, K. "The Sarasota Mystery," Popular Electronics, March, 1966, pp. 50 - 53.